Available online at www.sciencedirect.com

SCIENCE DIRECT®

ELSEVIER

Microelectronic Engineering 82 (2005) 1–11

MICROELECTRONIC ENGINEERING

www.elsevier.com/locate/mee

Simultaneous UV embossing method for fabricating two parallel organic layers with different hydrophilicity

Yong Young Park [a], Hansol Cho [b,*], Young Mok Son [b], Joon-Yong Park [b], Lyongsun Pu [b], Sang KeeYoon [c], Yoon Shik Hong [c], Hyun Kee Lee [d]

[a] *Nano Fabrication Center, Samsung Advanced Institute of Technology (SAIT), Republic of Korea*

[b] *Flexible Display Program Team, Materials and Devices Research Center, SAIT Mt. 14-1, Nongseo-Ri, Giheung-Eup, Yongin-Si, Gyeonggi-Do 449-712, Republic of Korea*

[c] *SOM Team, Central Research Institute, Samsung Electro-Mechanics Co. Ltd. (SEMC), Republic of Korea*

[d] *eMD Laboratory, Central Research Institute, SEMC 314, Metan 3-Dong, Paldal-Gu, Suwon-Si, Gyeonggi-Do 442-743, Republic of Korea*

Received 10 November 2004; received in revised form 21 January 2005; accepted 7 February 2005
Available online 24 May 2005

Abstract

We developed a simultaneous UV embossing method to fabricate bank-shaped, two parallel layers with different surface properties in a one-step processing using the mold having loop-shaped protrusions. In conjunction with ink-jet technology, the molded pattern could be used as barrier ribs for particular flat panel displays. We choose the layer materials so that the bottom ink-philic one absorb jetted ink and the top ink-phobic one expel jetted ink. Therefore, the structure prevents ink from staining the barrier ribs' surface and from mixing between adjacent pixels. The structure could be an effective barrier ribs for manufacturing of color filter of a liquid crystal display or light emitting layer of an electroluminescent display with high throughput.

Keywords: UV embossing; Barrier rib; Protrusion; Ink-jet; Hydrophilicity

1. Introduction

Recently, the organic light emitting display (OLED) have attracted enormous research interest and boosted industrial activity. They are a strong candidate for advanced flat panel display (FPD) in the near future because of their fascinating

* Corresponding author. Tel.: +82 31 280 6758; fax: +82 31 280 6725.
E-mail address: hansol@samsung.com (H. Cho).

0167-9317/$ - see front matter
doi:10.1016/j.mee.2005.02.008

properties; brightness, wide viewing angle, fast response time, low power consumption, emission spectra cover the entire range of visible light and so forth [1]. There is a possibility they can be used for flexible displays in a rolled form and on curved surfaces, even on the surface of cloth as a wearable display [2]. Therefore, it is plausible that OLED may be the most competitive FPD industry with current leading FPD one, liquid crystal display (LCD) in the near future. However, their success or even survival might strongly depend on a decrease in cost and an increase in display quality such as color purity or long-life time.

The success of large FPD in the field of PC monitors and TVs strongly depends on how we increase the mother glass size and lower the manufacturing and material cost. As a result, recent advances in the ink-jet technology, which originally developed as a printing technology, have taken some of the attention away from the display industry [3]. For LCD, the adaptation of low-cost ink-jet technology for color filter fabrication is strongly being considered [4,5] because it is scalable to large-size mother glass and economical in the material cost. On the basis of this standpoint, the ink-jet technology can also be used in polymer light emitting display (PLED) because PLED is capable of a soluble process.

When we use such ink-jet technology in FPD fabrication, it is inevitable to make the barrier rib on the substrate before ink-jetting step [6,7]. For example, the bank-shaped structure for a color filter of an LCD fabricated by photolithography is shown in Fig. 1. To prevent jetted ink from mixing with adjacent pixels and from remaining on the rib's surface, the bottom layer should be able to absorb ink and the top layer should be able to expel ink.

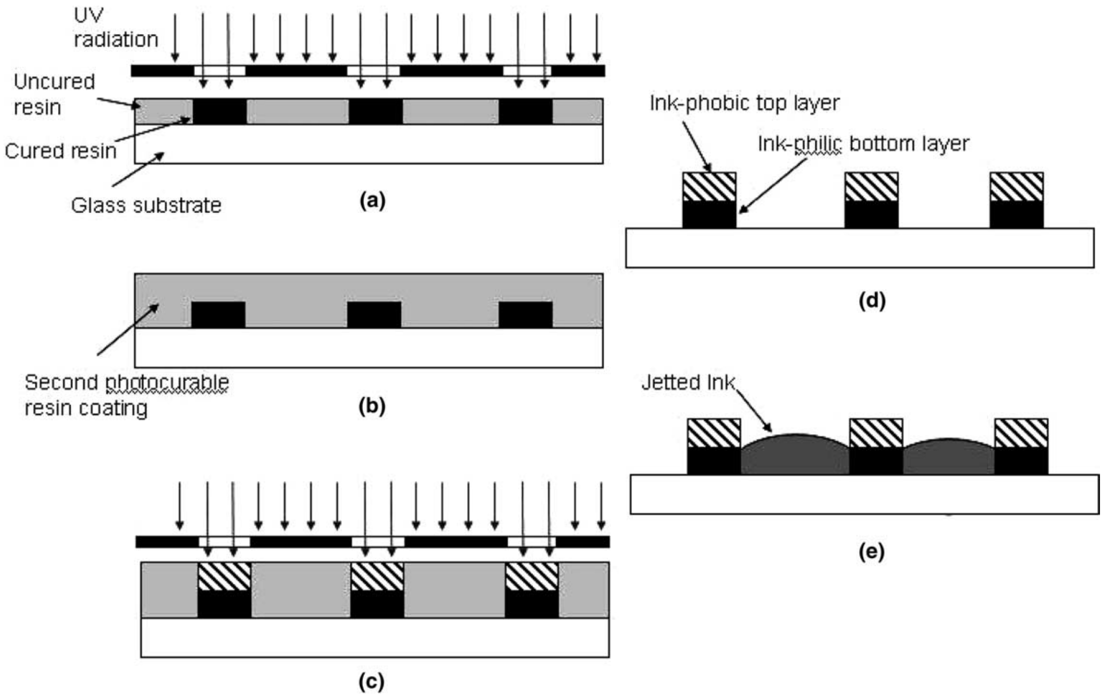

Fig. 1. Conventional manufacturing method and preliminary function of the barrier rib for a flat panel display that uses ink-jet technology. (a) Spin-coating of ink-philic, photocurable resin on a glass substrate and ink-philic bottom structure formed by UV exposure, (b) thick coating of ink-phobic photocurable material, (c) second photo process for ink-phobic barrier rib formation, (d) fabricated barrier rib structure consisting of two parallel layers after wet etching of uncured resin and (e) final shape of ink-jetted flat panel display.

However, the fabrication procedure is somewhat complicated. For example, to make a barrier rib structure like the one shown in Fig. 1 by means of a conventional photo resist technique, we have to repeat spin coatings, mask alignments, UV exposures and wet etching processes two times to fabricate the dual layers having different surface properties. The mask aligning is particularly bothersome and timeconsuming. The main aim of this work is to simplify the fabrication by using a new and effective process that includes just a single embossing and UV exposure step.

For this, embossing technique is considered. Often called the imprinting technique, the embossing technique uses a hard mold with protruded patterns defined on the surface of the mold, and these patterns even in a nanometer scale are imprinted onto a substrate's polymer layer cast [8]. Unlike conventional embossing processes that are usually achieved by applying pressure to a single photo curable resin film (UV embossing) or at a temperature higher than the glass transition temperature of a single polymer film (thermal embossing), our new process requires just one embossing procedure to fabricate dual layers with different surface properties. For this purpose, we use two deformable (flowable), immiscible materials as barrier rib components that differ greatly in viscosity. In the next section, we will deal with the principles of our method in more detail.

2. Simultaneous embossing concept of two parallel layers of different viscosity and hydrophilicity

In a conventional embossing process, the surfaces of the protrusions are flat. In most cases, the normal stress effect of viscous non-Newtonian fluid squeezes the flow between parallel plates; and this effect even works for viscoelastic polymeric fluid. As a result, this process is widely used for understanding the rheological characteristics of the embossing process [9,10]. On the basis of our new concept of embossing dual layers, we prepared a mold that had a triangular loop-like surface on each protrusion as shown in Fig. 2. The exterior angle θ is 15°.

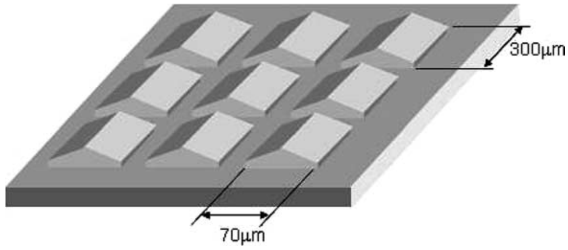

Fig. 2. Three-dimensional shape of the mold that has a triangular loop-like surface on each protrusion.

The most basic prerequisites of our process are that the two resins must be immiscible, and different in viscosity and hydrophilicity as illustrated in Fig. 3. The surfaces of the protrusions were triangular with a small angle, θ, to make the lateral squeezing flow (indicated by white arrow) in the top layer. We achieved this flow by pressing the mold perpendicularly so as not to remain the top resin of the low viscosity on top of the bottom layer after full embossing. When the layers of different viscosity are pressed at a speed shorter than the longest relaxation time of the viscous (strictly speaking, viscoelastic) bottom layer, the top layer of very low viscosity flows as a result of the squeezing between the mold surface and the lower layer, which acts as a solid.

To analyze this behavior, we referred to the concept of the Deborah number ($De = \tau_{\text{fluid}}/\tau_{\text{exp}}$), a dimensionless number that characterizes the flow of the material [11]. *De* is a ratio of the relaxation time of the intrinsic material fluidity and the time of the event or experiment. It therefore measures the relative strength of the elastic and convective effects of soft materials against external motion, particularly with respect to whether the soft materials act as a fluid or (elastic) solid. *De* of the top layer for a typical case of unpolymerized monomer, which is purely a viscous and Newtonian fluid, definitely goes to zero unless the time scale of the experiment is larger than the relaxation time of a small molecule in the order of picoseconds. To define the appropriate relaxation time of the bottom layer, we need the viscosity and elastic modulus under a low shear rate because the longest relaxation time is the ratio of viscous and elastic moduli. A typical bottom layer consists of photo

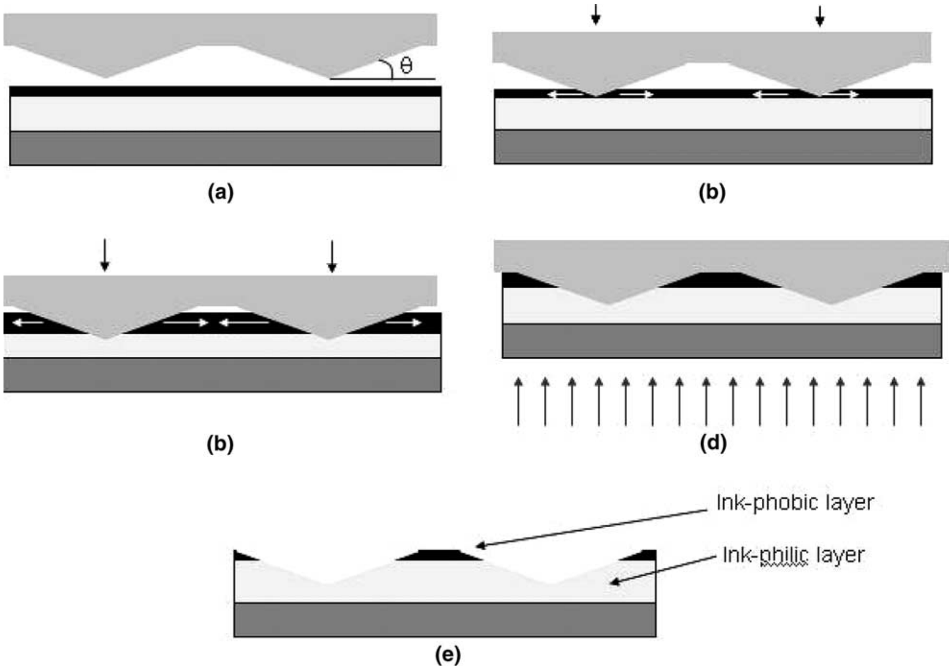

Fig. 3. Schematics of the simultaneous UV embossing method of two parallel layers. (a) Dual coating of high-viscosity and low-viscosity layer on glass substrate, (b–c) carefully pressing a mold that had a triangular loop-like surface on each protrusion, (d) curing of two layers by UV radiation onto the substrate side and (e) final structure of two parallel layer having ink-philic and ink-phobic layers by our method.

resist material comprised mainly of a linear polymer and a monomer that is photo crosslinkable and multifunctional after spin coating. However, if we make a simple assumption that the thermoplastic polymer is under or around the glass transition temperature, then the typical relaxation time is at least in the order of 1 s according to the definition of glass transition.

For a squeezing flow, the experimental time scale is usually half the time required for the mold and substrate to come together [12]. For a typical embossing process, the pressing speed of V is in the order of 10 μm/s and the gap between the mold and the substrate of H is in the order of 10 μm. By considering these factors, we get

$$De_{\text{bottom}} > \frac{1}{1/2(H/V)} = 2.0. \tag{1}$$

Given that $De_{\text{top}} = 0$ and Eq. (1) is the extreme low limit of De_{bottom}, the top layer acts as a liquid and the bottom one acts as a solid in our embossing concept. However, we must be able to deform the bottom layer by pressing the mold.

The Reynolds number (Re) is another dimensionless number that is needed to make clear the flow stability of the top resin layer of, for example, $\eta = 10$ mPa s. The calculated result is

$$\begin{aligned} Re_{\text{top}} &= \frac{HV_\rho}{\eta} \\ &\sim \frac{(10^{-5}\ \text{m})(10^{-5}\ \text{ms}^{-1})(10^{3}\ \text{kg/m}^{3})}{(10^{-2}\ \text{kg m}^{-1}\ \text{s}^{-1})} \\ &= 10^{-4}, \end{aligned} \tag{2}$$

which is low enough to assume an absence of vortex, turbulence or a secondary flow in the top layer. In other words, the flow is a laminar flow, and thus there is no mixing between top and bottom resins. The process also lowers the possibility of the presence of a residual top resin on the outer surface of the bottom layer. Even

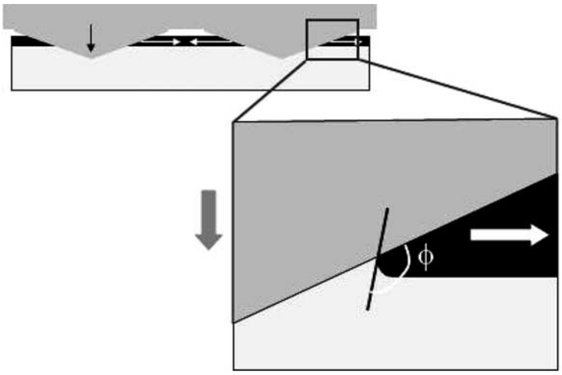

Fig. 4. Contact angle formation during embossing step.

though the viscosity of the top layer is very low, Re_{top} is not high due to the slow embossing speed.

The next issue is the hydrophilicities of the resins before and after UV curing. A key material property to determine the shape of the fluid–fluid interface is the contact angle, the angle formed at the intersection of the solid and the fluid–fluid interfaces. The static contact angle between the smooth solid surface (S) and two immiscible layers (L_1, L_2) is described by Young's equation [13]

$$\cos\phi = \frac{\gamma_{SL_1} - \gamma_{SL_2}}{\gamma_{L_1L_2}}, \tag{3}$$

where γ_{ij} is the surface tension of the interface between component i and j. The cohesive forces between molecules are responsible for the surface tension. We would like to make γ_{SL_1} to be low by selecting mold surface S, and bottom layer material L_1, of either same hydrophilicity, and γ_{SL_2} to be high by selecting a top layer material L_2 of the opposite hydrophilicity. Therefore the value of $\cos\phi$ in Eq. (3) tends to be negative or at least small, that is, $\phi \geqslant 90°$ as illustrated in Fig. 4. In other words, the top layer does not wet either mold surface or bottom layer sufficiently, whereas the bottom layer wets the mold surface well.

3. Preparation of the mold

A new method of fabricating Si mold whose protrusion surface is of triangular loop-shape is developed. It exploited a microloading effect of inductively coupled plasma (ICP) dry etching to form an inclined surface on Si substrate. In our case, we controlled the depth of the etching by using the difference in the gaps of the pre-patterned photo resist. The size of the difference in the gaps induces the difference in the depths of the dry etching due to the loading effect. A schematic illustration in Fig. 5 shows the preparation steps for fabricating the Si mold with protrusion pixel units in detail. Fig. 5(a) shows a predetermined photo resist pattern on the Si substrate. We formed the photo resist pattern on the Si wafer with controlled critical dimensions considering the loading effect. The gaps between the patterns were 2, 3, 4.5, 6.5 and 9.0 μm, respectively. This data is based on the depths of the etching after the preliminary dry etching experiments. STS ICP etcher (HR model) was used to form the Si mold with inclined surface. A typical process for forming high aspect ratio (HAR) structure, Bosch process, which fabricates HAR structure by repeating etching and deposing cycles, was adopted [14]. Since microloading effect influences the etch rate, the etched depth is dependent on the photo resist gap size. Typical etch rates were 0.63 μm/min for 6 μm gap and 0.84 μm/min for 9 μm gap [15]. After conducting ICP dry etching, we obtained Si structure with valleys of controlled depths, as illustrated in Fig. 5(b). We removed the photo resist that acted as a mask by wet etching (Fig. 5(c)). The scanning electron microscopy (SEM) images were shown in Figs. 6(a) and (b), both of which correspond to Fig. 5(c). We further carried out wet oxidation process at over 1000 °C for 4 h. It turned the 2 μm thick dummy Si blocks into silicon dioxide. All silicon oxide dummy blocks were removed by wet process using buffered oxide etcher (DI water/HF = 6:1) [16]. Therefore, stair-shaped inclined surface was obtained as illustrate in Fig. 5(d).

To make the surface smooth, further planarization of the surface of the mold was performed by repeating several wet etching steps with a tetramethyl ammonium hydroxide (TMAH) solution at 80 °C for 3 min. The irregular tips left after removing dummy blocks were removed

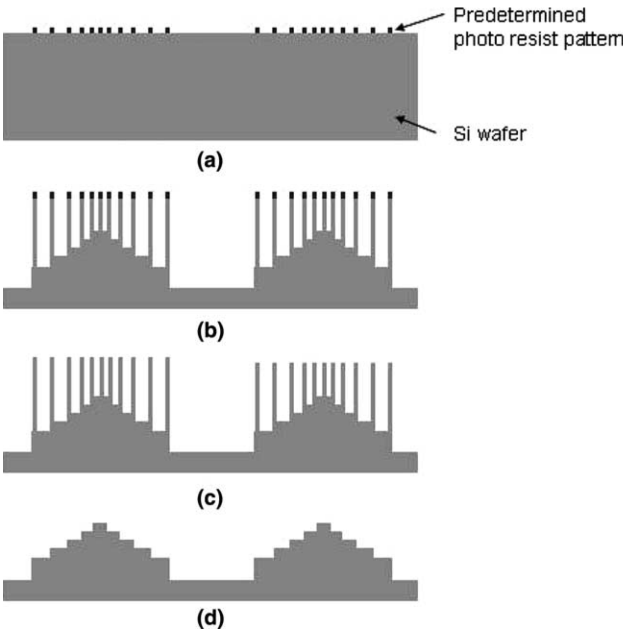

Fig. 5. Schematic illustration of the mold preparation steps. (a) patterning of predetermined photo resist structure on the Si substrate, (b) anisotropic dry etching which makes the depth difference, (c) removal of photo resist, (d) obtained Si mold which has a rough loop-like shape on each protrusion after removal of unnecessary dummy blocks by oxidation and wet etching. Final mold structure shown in Fig. 4 can be obtained by further planarization by repeated wet etchings with a tetramethyl ammonium hydroxide solution.

successfully by the TMAH treatments and hence the surface of loop-like protrusion of our Si mold was sufficiently smoothed. The final mold's SEM image and a three-dimensional confocal laser scanning microscope image after planarization were shown in Figs. 6(c) and (d).

Finally, we coated super-hydrophobic polymer film (typically ~30 nm thick) on the surface of the Si mold by dip coating with Zonyl® TC-10, by courtesy of Dupont Japan. The contact angle of the water on the coated surface was at least 110°.

4. Results and discussion

For the top layer of the purely viscous, hydrophilic material, we prepared 2-hyroxy(ethylene methacrylate) (HEMA) purchased from Aldrich, which contains a UV initiator (Irgacure 184 from Ciba Specialty Chemical). For the bottom layer of the highly viscoelastic, hydrophobic material, we used ORMOCER®, a transparent, UV-curable, organic-inorganic hybrid polymer, which we purchased from Micro Resist Technology, Germany. To measure the contact angle of these materials, we used sessile water drop measurement. The water contact angle of poly(2-hyroxy(ethylene methacrylate)) (PHEMA) (60°) was reported by Mora et al. [17]. ORMOCER is a hybrid material that contains silicon and acrylic multifunctional monomers. We added small amount of tetra-fluoropropyl methacrylate (~5 wt%) to make bottom layer's surface more hydrophobic and maintain its viscous characteristics. Its contact angle after UV curing was about 85° which is slightly larger than that of PMMA.

In our system, it is important to analyze the dynamic contact angle while pressing the mold (squeezing the two immiscible layers) because the shape change of the interface might strongly

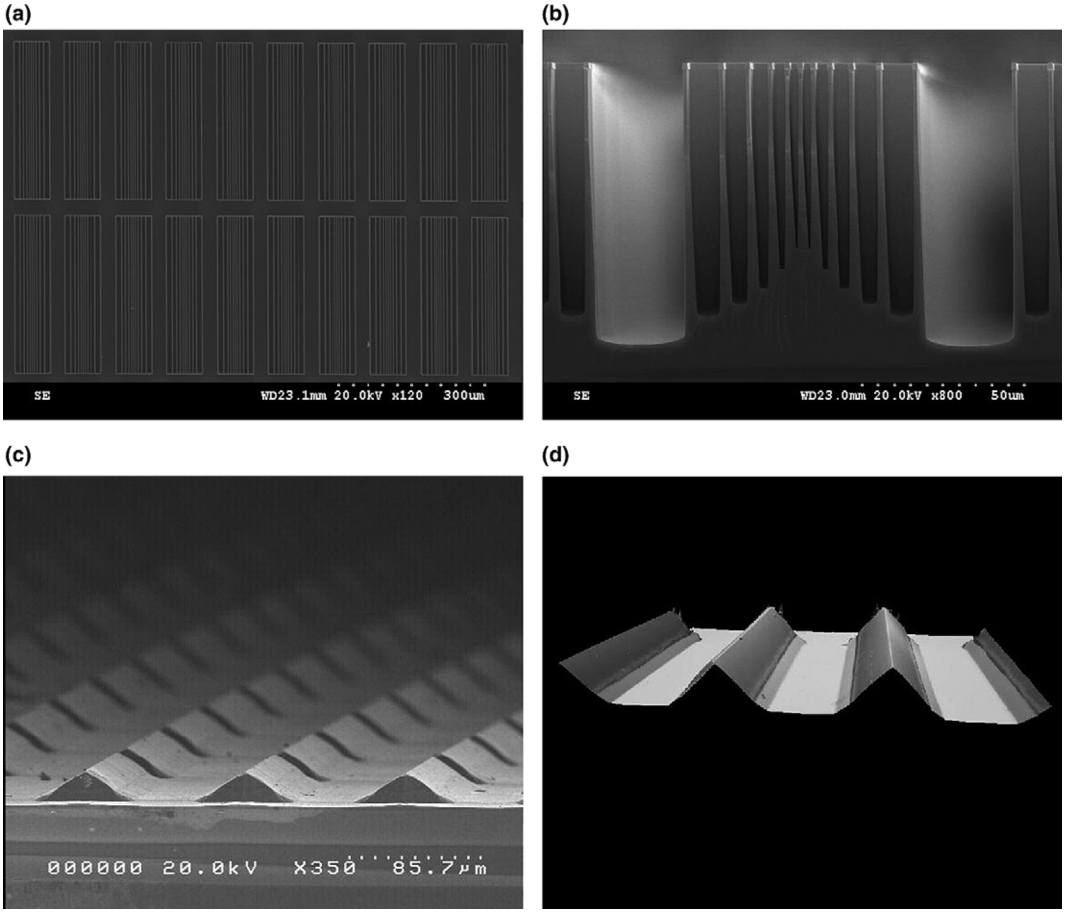

Fig. 6. SEM images of (a) a pattern corresponding to Fig. 5(c) from the top view, (b) a pattern corresponding to Fig. 5(c) from the section view, (c) the final mold after removal of unnecessary dummy blocks, and (d) a confocal laser scanning microscope image of final mold.

influence on the presence of top resin residue on the surface of bottom layer before UV curing, however, its theoretical analysis is beyond our research scope because of the difficulty in measurement of layers' liquid states before UV curing. This might be another interesting research topic when associated with squeezing flow problem. Instead, we experimentally show the clear separation of each layer after mold pressing and UV curing.

In preparing the two-layers with different viscosity and hydrophilicity, we dropped the ORMOCER resin on a soda lime glass of 0.7–1.1 mm in thickness, and then spin-coated at a rotation speed of 2000–3000 rpm for 30 s to ensure the bottom resin layer had a thickness of 8–15 μm. The ORMOCER layer is sufficiently viscous (about 5000 mPas after spin coating measured by ARES rheometer in a cone-and-plate geometry at a shear rate 0.1 s^{-1}) even though it has not been cured. We dropped several droplets of HEMA mixture on the uncured ORMOCER bottom layer, and then pressed our mold on the layers with a pressure of 5 kgf/cm^2. Subsequently, the UV light was radiated on the back face of the soda lime glass for 3–5 min. After finishing the curing, we released the mold and observed the resultant pattern with the aid of an optical microscope, as shown in Fig. 7(a), and a scanning electron microscope (SEM), as shown in Fig. 7(b). Its surface was observed using confocal laser scanning microscope (Keyence, VK-9500). As shown in Fig. 8(a), a smooth and clear surface was obtained. For comparison, another sample was prepared by leaving the pressed layers for 30 min quiescently and then curing by UV radiation. Its surface was a little bit wrinkled as shown in Fig. 8(b). This wrinkling surface might be induced by slight mixing of top and bottom resins in the interface during intermediate duration of 30 min because ORMOCER contains an acrylic ingredient that has some affinity to HEMA's methacrylic unit even though they are apparently immiscible. Therefore, instantaneous coating, pressing and UV radiation are preferential for production of smooth surface.

To analyze the presence of top resin on the bottom layer of the pattern, we conducted micro Raman image mapping using a Nanofinder 30

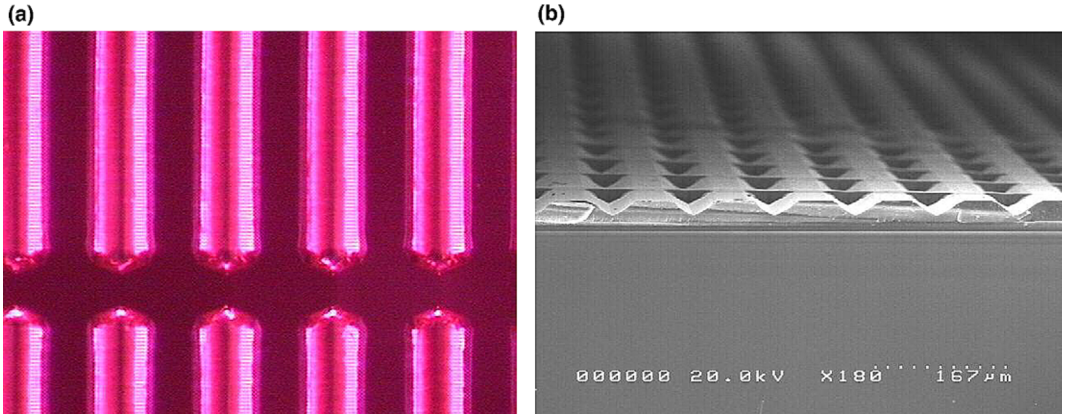

Fig. 7. (a) Optical microscope and (b) SEM images of the PHEMA-ORMOCER dual layer pattern.

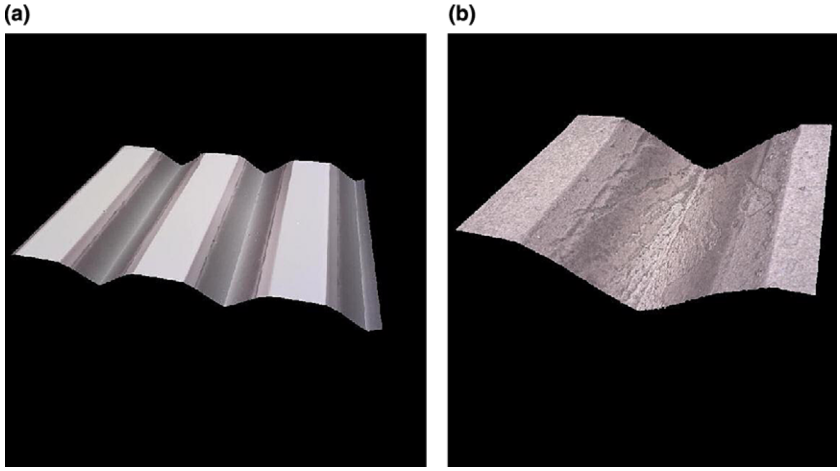

Fig. 8. Comparison of confocal laser scanning microscope images of samples for (a) instantaneous pressing and UV curing and (b) UV-cured after for 30 min duration.

Tokyo Instrument. The experimental conditions included 100 points along one dimension, 100 scanning steps, a shift speed of 2 μm/s, and an exposure time of 0.5 s. The first step was to find a distinctive peak of ORMOCER after the UV curing. Fig. 9(a) shows that the ORMOCER has distinct shift peak at around 980 cm^{-1}. Next, we scanned the sample. Figs. 9(b) and (c) show the results of the two-dimensional image mapping. In the top layer region, very low level of the Raman peak was observed, which implies the absence of ORMOCER resin on the top layer of our sample. In the caved region, on the other hand, there was a strong Raman shift peak at 980 cm^{-1}, which implies an absence of PHEMA in the region of the bottom layer. This result strongly indicates that our method of UV embossing sufficiently separates each layer on the top and bottom regions.

Because ORMOCER contains an acrylic monomer, it does not make a clear interface in SEM images between the top and bottom layer with PHEMA, even though we rapidly did the embossing and UV radiation. We therefore prepared another dual layer pattern by simultaneous thermal crosslinking of polydimentyle (PDMS) as a bottom layer and UV curing of HEMA as a top layer to show that our method separates the top and bottom layers clearly. In case of PDMS, the water contact angle is about 95°. In Figs. 10(a) and (b), the discrete interface is indicated by an arrow. Thus, it could be concluded that clearly separated two parallel layers possessing different hydrophilicity was successfully fabricated by our new embossing method.

Ink-jet printing using our bank-shaped patterns is beyond the scope of this report. However, we would like to mention the problems associated with jetting and drying on the basis of simple physical intuition: The droplet shape of jetted ink (hydrophobic ink in our case) might be determined by the bank shape and interface properties of the top and bottom layers [18]. Moreover, during drying, the thickness of the solute's residue is strongly affected by the local flux of the solvent and the pinning position but hardly influenced by the gravity or geometrical shape of the bottom. Therefore, neither jetting nor drying is thought to be influenced by the caved shape of our method unless the exterior angle of protrusion, is high.

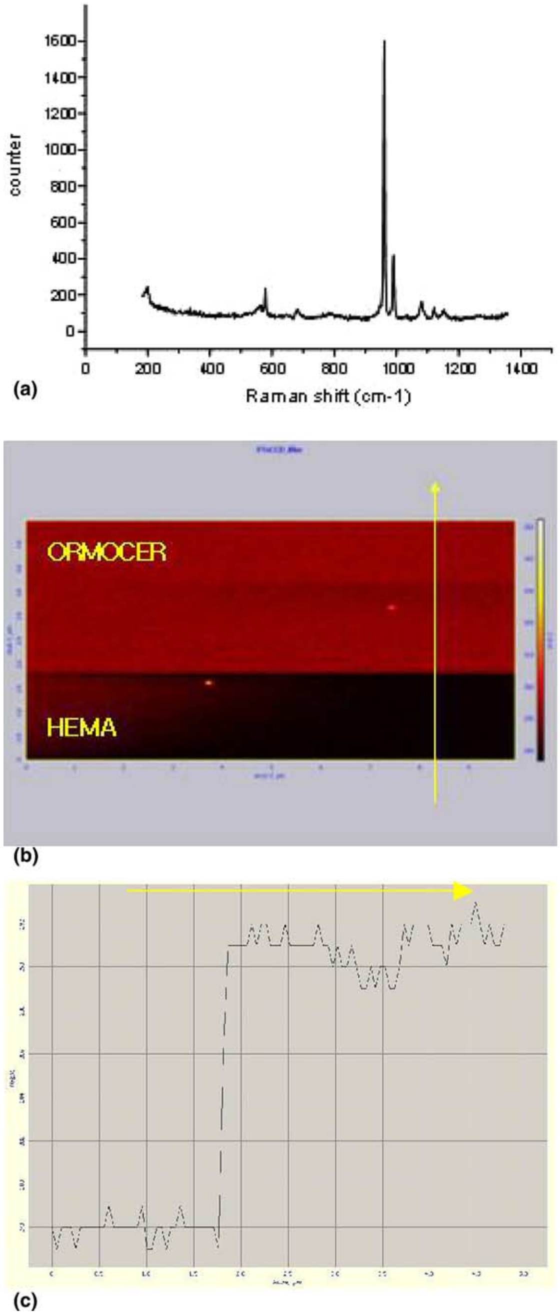

Fig. 9. Micro Raman image mapping experiments. (a) Raman shift of ORMOCER, (b) top view of intensity profile, (c) intensity profile of ORMOCER Raman peak at 980 cm^{-1}.

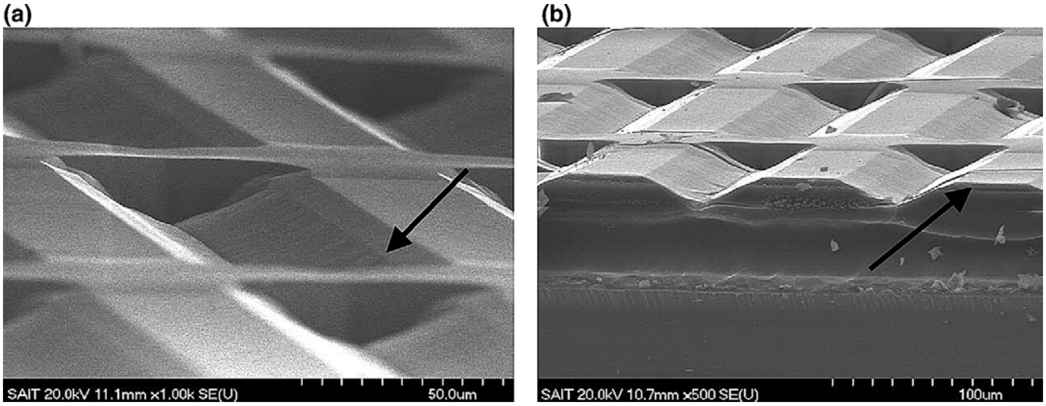

Fig. 10. SEM images of the PHEMA-PDMS dual layer pattern.

5. Conclusions

We successfully fabricated clearly separated two parallel layers in just one embossing process. Our fabrication method has great merit and potential because it is easy, inexpensive, expandable to a flexible substrate, capable of repeated embossing for a large pattern with LCD color filters or PLED that use ink-jet technology. In contrast, conventional methods of fabricating barrier ribs involve a multiple coating-mask, UV alignment and exposure-and-etching processes for masking with a pattern. Moreover, the two-layers with different hydrophilicity are also well fabricated. In our opinion, the ink-jetting of either a color filter or light emitting materials on the slightly caved surface of the banks would not give rise to serious problems if the exterior angle of protrusion of the triangular loop-shaped mold is sufficiently small.

Acknowledgements

The authors thank Dr. Seung Jin Lee of Dupont Korea and Mr. Takashi Kuno and Dr. Mureo Kaku of Dupont Japan for their preparation of the hydrophobic coating of Zonyl® TC-10 on our Si mold.

References

[1] V.G. Chigrinov, Liquid Crystal Devices: Physics and Applications, Artech House, Boston, 1999.
[2] J. Shinar, V. Savvateev, Introduction to organic light-emitting devices, in: J. Shinar (Ed.), Organic Light-emitting Devices, a Survey, Springer-Verlag, New York, 2004.
[3] M. Grove, D. Hayes, R. Cox, D. Wallace, J. Caruso, M. Hampden-Smith, T. Kodas, K. Kunze, A. Ludviksson, S. Pennino, D. Skamser, in: Proceedings, Display Works '99, San Jose, Feb., 1999.
[4] O. Mamoru, Y. Yuji, S. Michiaki, NEC, Jap. Patent (2001) 042313A.
[5] S. Shoji, T. Hideaki, Y. Ryuichi, S. Masaji, O. Takeshi, Canon Inc., Jap. Pat. (2000) 089022A.
[6] M. Fleuster, M. Klein, P.v. Roosmalen, A.d. Wit, H. Schwab, SID Symp. Digest 35 (2004) 1276.
[7] B.-J. de Gans, P.C. Duineveld, U.S. Shubert, Adv. Mater. 16 (2004) 203.
[8] S.Y. Chou, P.R. Krauss, P.J. Renstrom, Appl. Phys. Lett. 67 (1995) 3114.
[9] H. Schulz, H.-C. Scheer, Microelectron. Eng. 56 (2001) 311.
[10] H. Schift, L.J. Heyderman, Nanorheology – squeeze flow in hot embossing of thin films, in: C.M. Sotomayor Torres (Ed.), Alternative Lithography – Unleashing the Potentials of Nanotechnologys, Kluwer Academic Publishers, London, 2004.
[11] R.B. Bird, R.C. Armstrong, O. Hassager, Dynamics of polymeric liquids, Second ed.Fluid Mechanics, vol.1, Wiley, New York, 1987.
[12] S. Middleman, Fundamentals of Polymer Processing, McGraw-Hill, New York, 1977.
[13] R. Probstein, Physicochemical Hydrodynamics, an Introduction, Wiley, New York, 1994.
[14] S.A. MeAuley, et al., Silicon micromachining using a high-density plasma source, J. Phys. D: Appl. Phys. 34 (2001) 2769.
[15] A. Rickard et. al., Characterisation and optimisation of deep dry etching for mems applications', in: SPIE Int'l Conf. on Microelectronic & MEMS Technologies, Edinburgh (UK), May 2001, 1.

[16] S. Wolf, R.N. Tauber, Silicon processing for the VLSI EraProcess Technology, vol. 1, Lattice Press, USA, 1986.
[17] M. Morra, C. Cassinelli, Biomed. Mater. Res. 29 (1995) 39.
[18] T. Kawase, H. Sirringhaus, R.H. Friend, T. Shimoda, Adv. Mater. 13 (2001) 1601.